Eur Radiol (2008) 18: 510–521
DOI 10.1007/s00330-007-0772-1

Julia Ley-Zaporozhan
Sebastian Ley
Hans-Ulrich Kauczor

Morphological and functional imaging in COPD with CT and MRI: present and future

Received: 8 March 2007
Revised: 26 August 2007
Accepted: 31 August 2007
Published online: 27 September 2007

J. Ley-Zaporozhan (✉) · S. Ley · H.-U. Kauczor
Department of Radiology (E010), German Cancer Research Center, Im Neuenheimer Feld 280, 69120 Heidelberg, Germany
e-mail: juliazapo@web.de
Tel.: +49-177-5141849

S. Ley
Department of Pediatric Radiology, Ruprecht-Karls-University, Im Neuenheimer Feld 153, 69120 Heidelberg, Germany

J. Ley-Zaporozhan
Department of Diagnostic and Interventional Radiology, Johannes Gutenberg-University Hospital, University of Mainz, Langenbeckstrasse 1, 55131 Mainz, Germany

Abstract Chronic obstructive pulmonary disease (COPD) is one of the leading causes of morbidity and mortality worldwide. COPD is defined by irreversible airflow obstruction. It is a heterogeneous disease affecting the airways (i.e. chronic bronchitis, airway collapse), the parenchyma (i.e. hyperinflation, air trapping and emphysematous destruction) as well as the vasculature (i.e. hypoxic vasoconstriction, rarefication and pulmonary arterial hypertension) with different severity during the course of the disease. These different aspects of COPD can be best addressed by imaging using a combination of morphological and functional techniques. Three-dimensional high-resolution computed tomography (3D-HRCT) is the technique of choice for morphological imaging of the lung parenchyma and airways. This morphological information is to be accomplished by functional information about perfusion, regional lung mechanics, and ventilation mainly provided by MRI. The comprehensive diagnostic possibilities of CT complemented by MRI will allow for a more sensitive detection, phenotype-driven characterization and dedicated therapy monitoring of COPD as presented in this review.

Keywords COPD · CT · MRI · Perfusion · Ventilation

Introduction

Chronic obstructive pulmonary disease (COPD) is one of the leading causes of morbidity and mortality worldwide. At present it is the fourth most common cause of death among adults [1]. COPD is characterized by airflow limitation that is not fully reversible. The airflow limitation is usually progressive and associated with an abnormal inflammatory response of the lung to noxious particles or gases. It is caused by a mixture of airway obstruction (obstructive bronchiolitis) and parenchymal destruction (emphysema), the relative contributions of which are variable [1]. Chronic bronchitis, or the presence of cough and sputum production for at least 3 months in each of two consecutive years, remains a clinically and epidemiologically useful term. Pulmonary emphysema is a pathological term and is defined by the American Thoracic Society as an abnormal permanent enlargement of the air spaces distal to the terminal bronchiole, accompanied by the destruction of their walls. In a simplified way, obstructive airflow limitation leads to air-trapping with subsequent hyperinflation and later destruction of the lung parenchyma. For severity assessment of COPD lung function tests such as forced expiration volume in one second (FEV_1), FEV_1/FVC (forced vital capacity) and diffusing capacity for carbon monoxide (DLco) are used. However, these are a

global measure of all changes occurring in COPD. Chronic hyperinflation impacts on diaphragmatic geometry with subsequent dysfunction due to dissociation of the breathing mechanics. The disease also affects the pulmonary arteries: intimal thickening, smooth muscle hypertrophy and inflammation were described finally leading to vascular remodelling [2]. The direct vascular changes and hyperinflation lead to the precapillary type of pulmonary hypertension [3].

This short introduction demonstrates the complex nature of the disease and the different effects which contribute to the clinical symptoms. A precise characterization of each component of the disease is desirable for therapy decisions and monitoring.

In contrast to spirometry, radiological imaging might allow for regional assessment of the compartments involved (i.e. airways, parenchyma and vasculature). Computed tomography (CT) is a long standing player in this field, with emphasis on structural imaging of lung parenchyma and airways. Magnetic resonance imaging (MRI) of the lung is hampered by several challenges: the low amount of tissue relates to a small number of protons leading to low signal; countless air-tissue interfaces cause substantial susceptibility artifacts as well as respiratory and cardiac motion [4]. The strength of the technique is the assessment of function like perfusion, ventilation and respiratory dynamics. The new diagnostic possibilities of CT complemented by MRI may enable a more sensitive detection and phenotype-driven characterization and therapy monitoring of COPD as presented in this review.

Parenchyma

CT

Accurate diagnosis and quantification of pulmonary emphysema in vivo is important to understand the natural history, assess the extent of the disease, and monitor therapy [5]. High-resolution CT (HRCT) is currently the method of choice for the non-invasive and sensitive assessment of pathological changes in emphysema and has been shown to correlate well with pathology [6, 7]. Using modern multislice CT (MSCT) technology the whole lung can be covered in a high-resolution mode and thin slice (1 mm or less) during a single breath-hold (3D-HRCT). Multiplanar reformations allow for easier perception of the distribution of emphysema.

The role of the distribution of emphysema on CT as a predictor of mortality is a hot topic and results are conflicting. One study reported a greater proportion of emphysema in the lower lung versus the upper lung to be predictive of mortality [8]. Other studies explored the influence of the distribution pattern of emphysema on different lung function parameters. A higher percentage of emphysema in the core was associated with a higher reduction in DL_{CO} (r^2=0.45) [9]. The contribution of emphysema in the core to pulmonary function (with FEV_1/FVC% r=0.66) may be larger than in the rind (r=0.56) [10].

Visual grading of the severity of emphysema showed less agreement with macroscopic pathology (r=0.4–0.5) than quantitative CT (r=0.6), the latter being less operator dependent [11]. Quantitative CT of emphysematous destruction consists of mean lung density, emphysema index, low end percentiles and other measures [6, 12–15]. Different thresholds have been investigated in the literature for thick and thin slices, ranging from -770 HU to -980 HU, revealing good correlation to pulmonary function test and pathology [6, 11–13, 15–18]. For thin slices the most often used threshold was -950 HU. Recently, a threshold of -960 or -970 HU has been suggested for MSCT; however, the images were reconstructed in an old-fashion HRCT method using a 10-mm interval gap, missing the chance for a truly volumetric analysis [15].

Density measurements are affected by technical parameters like reconstruction algorithm and slice thickness [19–21], and for follow-up examinations these parameters need to be kept constant. It is important to note that the tube current-time product can be reduced to 30-20 mAs without significant effects on emphysema quantification [21, 22].

Analysis of expiratory CT scans showed better correlations with pulmonary function test results than inspiratory scans: emphysema index with FEV_1 % predicted (r^2=-0.83 vs -0.6) [17] and emphysema volume with intrathoracic gas volume (r=0.88 vs0.83) and residual volume (r=0.93 vs 0.88) [18].

The pure evaluation of the emphysema index can be improved by an analysis of the hole size, e.g. using distribution of clusters of emphysematous volumes (Fig. 1) [18, 23]. Beyond analysis of volume clusters, 3D-HRCT datasets allow for advanced texture analysis, which might improve early detection [24], as such 3D textural features could discriminate the subtle differences between smokers and non-smokers both with normal lung function tests [25].

MRI

Proton MRI of the lung is hampered by low signal, which is even more pronounced in COPD patients as there is loss of tissue and reduced blood volume (Fig. 1). The extent of hyperinflation and hypoxic vasoconstriction is directly associated with the loss of signal [26]. Thus, until now MRI of the pulmonary parenchyma has only been successfully applied to diseases with an increase of tissue and signal, such as pulmonary nodules and masses [27]. While emphysematous destruction can hardly be diagnosed by a loss of signal, it is much easier to detect hyperinflation just by the size or volume of the thorax.

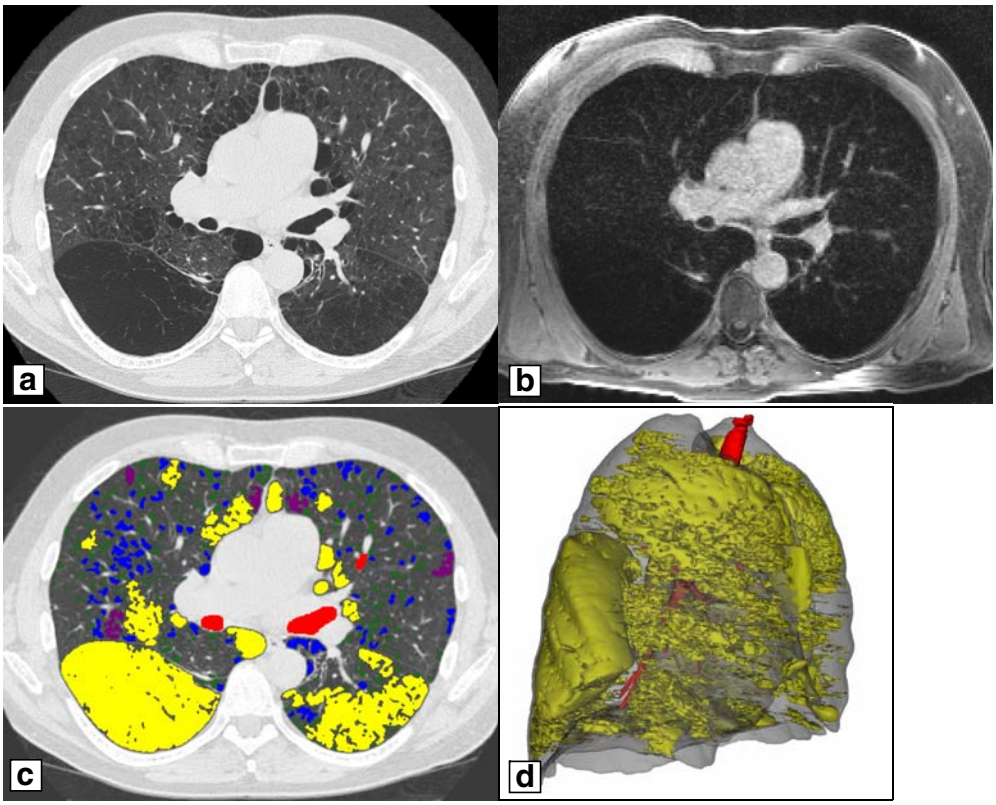

Fig. 1 Severe panlobular emphysema in the lower and centrilobular as well as paraseptal emphysema in the upper lobes. **a** 3D-HRCT shows the typical morphological features of these subtypes of emphysema. **b** The corresponding T1-weighted axial GRE (VIBE) post-contrast MR image shows a general signal loss in the lower lobes on MRI reflecting destruction of the parenchyma and rarefication of the pulmonary vasculature. Please note the difference in signal intensity between the centrilobular and panlobular emphysema. The colour-coded overlay of the 3D-HRCT (**c**) shows the size distribution (cluster) of the emphysematous areas (large clusters in *yellow*, intermediate in *purple* and small in *blue and green*). Colour-coding of all emphysematous areas (emphysema index) in the 3D volume (**d**) illustrates the heterogeneous distribution which can be used for planning locoregional therapies, such as lung volume reduction surgery

Airways

Several pathological studies have shown that a major site of airway obstruction in patients with COPD is in airways smaller than 2 mm internal diameter [28]. The 2 mm airways are located between the fourth and the 14th generation of the tracheobronchial tree. Airflow limitation is closely associated with the severity of luminal occlusion by inflammatory exudates and thickening of the airway walls due to remodelling [29]. Severe peripheral airflow obstruction can also affect the proximal airways from subsegmental bronchi to trachea. For assessment of tracheal instability cine acquisitions during continuous respiration or forced expiration either by CT or MRI are recommended (Fig. 2) [30, 31].

CT

CT can characterize anatomic details of the lung as small as 200–300 μm, which correspond to approximately the seventh to nineth bronchial generation [32]. On the basis of high resolution volumetric datasets, sophisticated post-processing tools will automatically segment the airways down to the eighth generation [33]. As a powerful adjunct to inspiratory scans, expiratory acquisitions reveal changes in lung attenuation related to air-trapping and pulmonary blood volume, and illustrate regional volumetric changes providing deeper insights into local hyperinflation and expiratory obstruction [18]. Since the severity of emphysema, as evaluated by CT, does not necessarily show a very good correlation with FEV_1 [13, 18], small airway disease appears to contribute more significantly to the airflow limitation in COPD. Regional air-trapping reflects the retention of excess gas at any stage of respiration as an indirect sign of peripheral airway obstruction. It is best detected on expiratory CT as areas with abnormally low attenuation [34]. Air-trapping is highly unspecific as it occurs under physiological conditions as well as in a variety of lung diseases, including emphysema, bronchiectasis, bronchiolitis obliterans and asthma [35].

Using HRCT images (with 10 mm gap) and visual assessment, bronchial wall thickness and the extent of emphysema were the strongest independent determinants of a decreased FEV_1 in patients with mild to extensive emphysema [9]. However, visual assessment of bronchial wall thickening is highly subjective and poorly reproducible [36]. Nakano et al. [37] were the first to perform quantitative measurements of airway wall thickening in COPD patients and reported a significant correlation between wall thickness of the apical right upper lobe bronchus and FEV_1% predicted. Due to technical limitations of HRCT, neither the generation of the bronchus measured could be determined nor measurements could be performed exactly perpendicular to the axis of the bronchus. The use of curved MPR from 3D-HRCT is a solution to

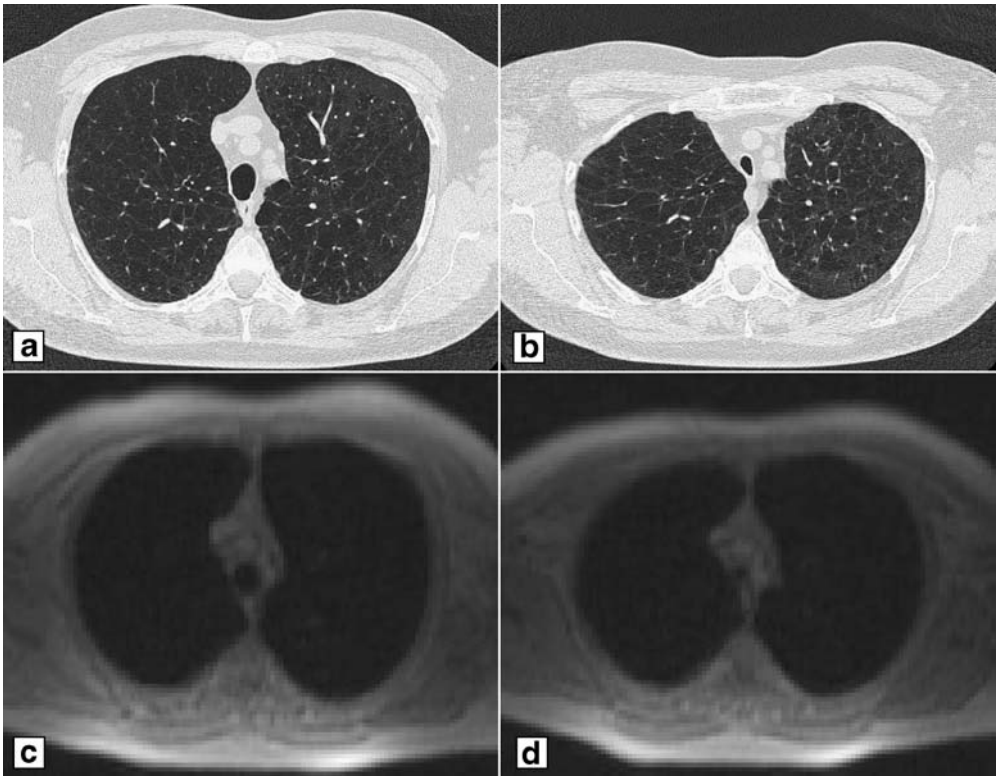

Fig. 2 A 56-year-old female patient suffering from COPD (FEV_1=0.96l/s, FEV_1 39% predicted). Cine-CT (*top*) and cine-MRI (FLASH 2D) (*bottom*) acquired during fast forced expiration (FEV1 manoeuvre) starting from maximum inspiration (**a**, **c**) to maximum expiration (**b**, **d**) both illustrating the tracheal collapse

accurately measure airway dimensions regardless of their course with respect to the transaxial CT scan (Fig. 3) [38]. Such measurements revealed high correlations between airway luminal area, and to a lesser extend for wall thickening, with FEV_1% predicted in patients with COPD. The correlation actually improved as airway size decreased from the third (r=0.6 for airway luminal area and r=0.43 for wall thickening) to sixth bronchial generation (r=0.73 and r=0.55, respectively) [38].

As the contributions of parenchymal changes and airway abnormalities to the overall airflow limitation will vary, 3D-HRCT may become the modality of choice for the differentiation between parenchymal and airway predominant disease, so-called phenotyping of COPD.

MRI

High spatial resolution is essential for visualization of the airways which can be achieved by a 3D volume interpolated gradient echo sequence (VIBE) with a voxel size of approximately $0.9\times0.88\times2.5$ mm^3. This technique showed a sensitivity of 79% and a specificity of 98% regarding visual depiction of bronchiectasis compared with CT [39]. The intravenous application of contrast material may improve the diagnostic yield of these T1-weighted sequences by a clearer delineation of vessels, hilar structures and inflammation within the bronchial walls. By T2- and T2*-weighted sequences, such as HASTE, MRI has unique capabilities to visualize inflammation, mucus, edema and fluid collections. The combination of T2-weighted and ce T1-weighted sequences may be an attractive alternative for imaging of airway inflammation without radiation (Figs. 1, 4) [40].

Perfusion

Gas exchange in the lungs is maintained by a balance between ventilation and perfusion. In patients with COPD, ventilation is impaired due to airway obstruction and parenchymal destruction. In regions with reduced ventilation hypoxic vasoconstriction occurs [41], leading to reduction of local pulmonary blood flow [42]. The reduction of the pulmonary vascular bed is related to the severity of parenchymal destruction [43]; however, the distribution of perfusion does not necessarily match parenchymal destruction (Fig. 5) [44, 45]. Conventional radionuclide perfusion scintigraphy has been used to assess these abnormalities, but it has substantial limitations with respect to spatial and temporal resolution. A superior technique is SPECT, which is rarely used as it is rather time-consuming and not routinely applied.

CT

Dynamic CT has been used to estimate arterial, venous, and capillary transit times as well as capillary flow

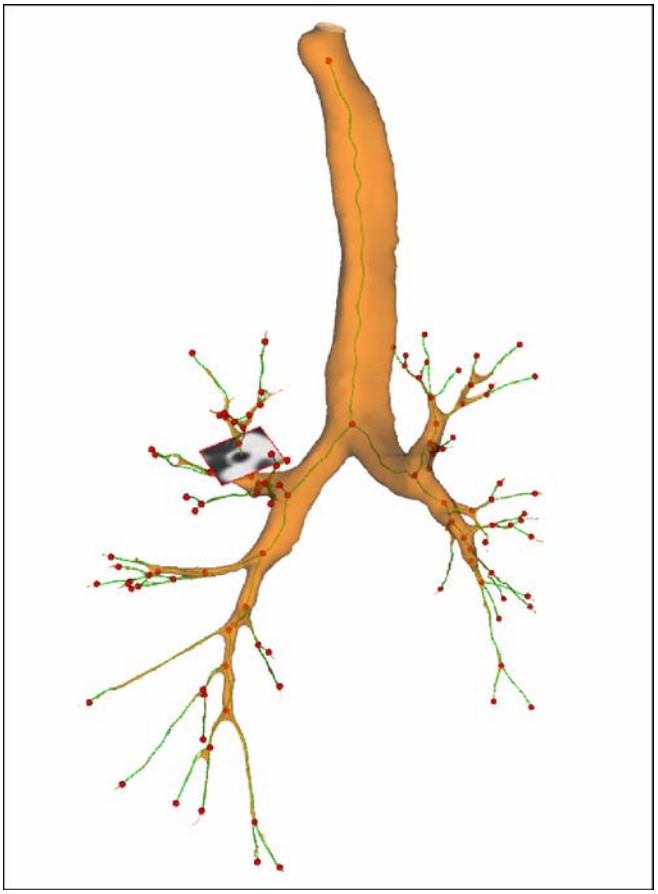

Fig. 3 3D volume rendering of tracheobronchial tree (*orange*), centerline (*green*) with branching points (*red*) and perpendicular image of the right upper lobe bronchus

distributions. Various approaches for determining blood flow and mean transit time have been described [46]. To date CT perfusion is mainly focused on the visualization of perfusion defects in pulmonary embolism or the characterization of lung tumours. No application in COPD patients has been reported so far.

MRI

Dynamic image acquisition during and after an intravenous bolus injection of a contrast agent (gadolinium-DTPA) allows for acquisition of volumetric perfusion weighted 3D datasets (FLASH 3D) with a high spatial resolution and the possibility for multiplanar reformation [47, 48]. In comparison with radionuclide scintigraphy MR perfusion shows a high diagnostic accuracy (90–95%) in detecting perfusion abnormalities [47]. Lobar and segmental analysis of the perfusion defects can be achieved [45]. In general, COPD patients with emphysema exhibit a low degree of contrast enhancement [49]. The distribution pattern is different from that in vascular obstruction. In a study with quantitative evaluation of 3D perfusion in patients with COPD, mean pulmonary blood flow (PBF), mean transit time (MTT), and pulmonary blood volume (PBV) were diffusely decreased and the changes were heterogeneous (Fig. 6) [50]. In expiration the physiological increase in blood volume is appreciated in normal lungs, while it remains low in emphysematous areas (Fig. 7).

Hemodynamics

Although pulmonary hypertension and cor pulmonale are common sequelae of COPD, the direct mechanism remains unclear [2]. In COPD patients the pulmonary vessels show a reduced or no capacity for vessel dilatation due to a defect in synthesis and/or release of nitric oxide. Prior to the onset of clinical symptoms patients exhibit signs of vascular bed obstruction and elevated pulmonary artery pressure, including pulmonary artery dilatation. Pulmonary hypertension is most often mild to moderate (mean pulmonary artery pressure in the range 20–35 mmHg) but it may worsen markedly during acute exacerbations, sleep and exercise [51]. Assessment of the pulmonary arterial pressure is necessary since COPD patients with severe pulmonary hypertension have a poor prognosis and need adequate treatment (including vasodilators) [51]. The value of echocardiography which is routinely used for this purpose is limited since the acoustic window patients with emphysema is narrow.

CT

Faster MSCT scanners allow for ECG gated acquisition of the entire thorax. This enables, beside the parenchymal analysis, evaluation of right ventricular function [52].

Fig. 4 Axial T1-weighted GRE (VIBE) post-contrast MR image showing bronchial wall thickening and enhancement within the right lower lobe (*circle*)

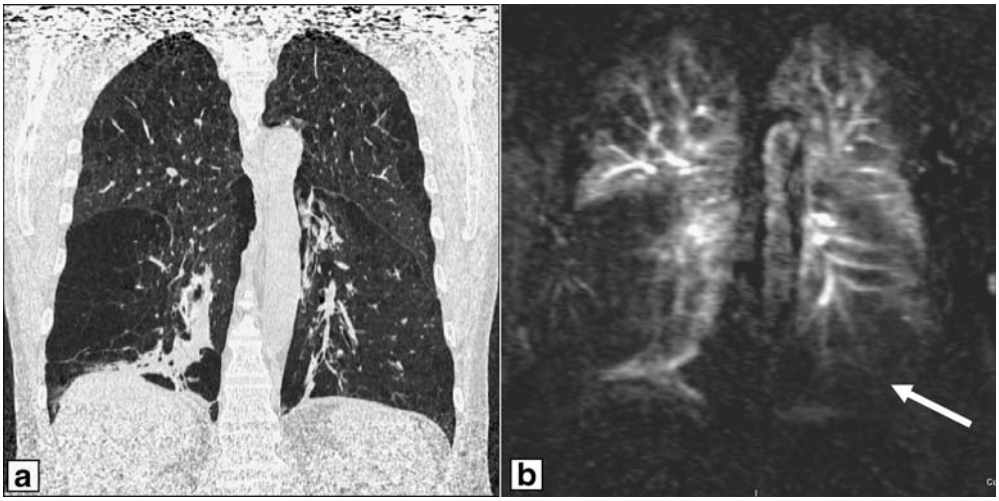

Fig. 5 Coronal CT reformat (**a**) and subtracted coronal contrast-enhanced MR perfusion image (10-mm MIP) (**b**), both acquired during an inspiratory breath-hold. Severe emphysema with right lung predominance and scar tissue of the right lower lobe on CT correspond to a loss of perfusion on MRI. A mismatch is found in the left lower lung where the perfusion is more reduced (*arrow*) than in the left upper lung which exhibits a similar moderate degree of centrilobular emphysema

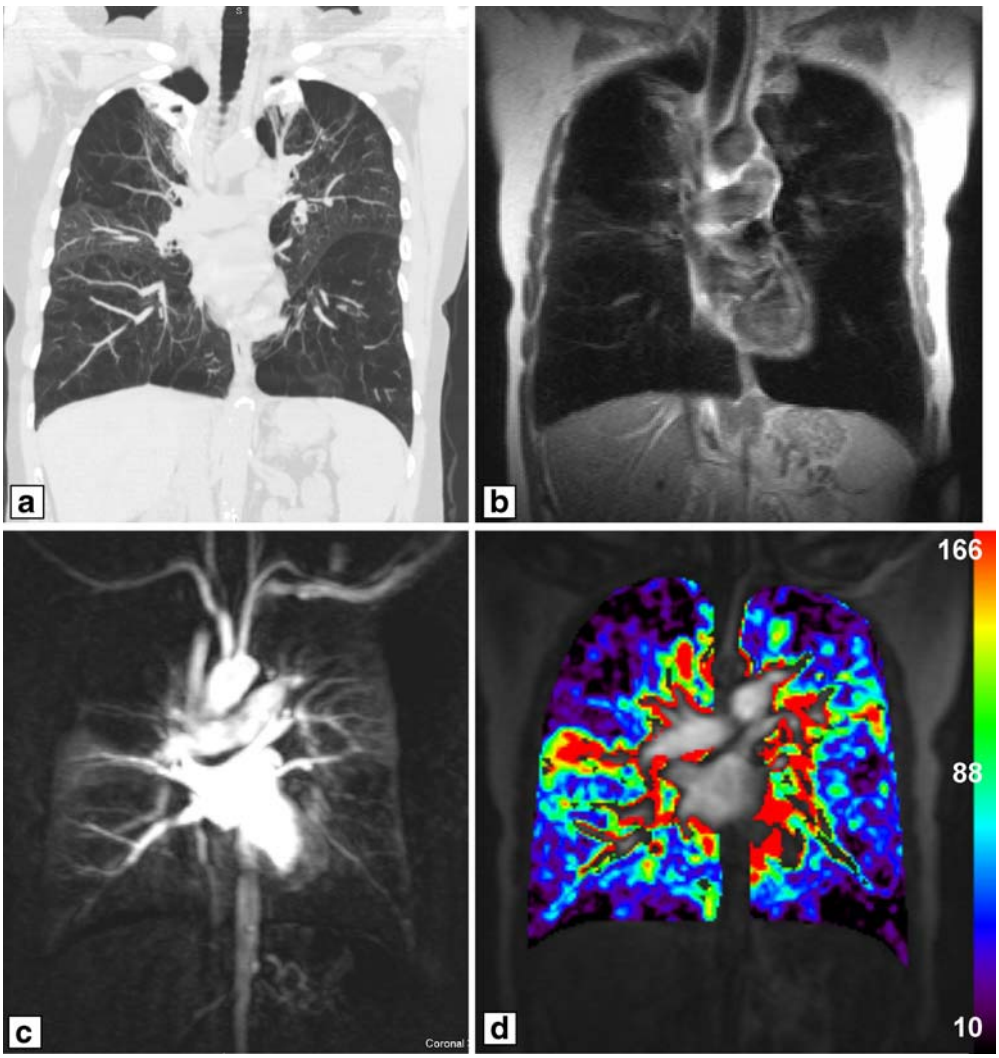

Fig. 6 Coronal CT (5-mm MIP) (**a**), corresponding T2-weighted coronal MR image (**b**) and ontrast-enhanced MR perfusion image (30-mm MIP) (**c**). Parameter map of quantitative analysis of MR perfusion shows the distribution of the pulmonary blood flow (**d**). Severe emphysema is nicely demonstrated on CT and MR with a match of severe destruction and reduction of pulmonary perfusion

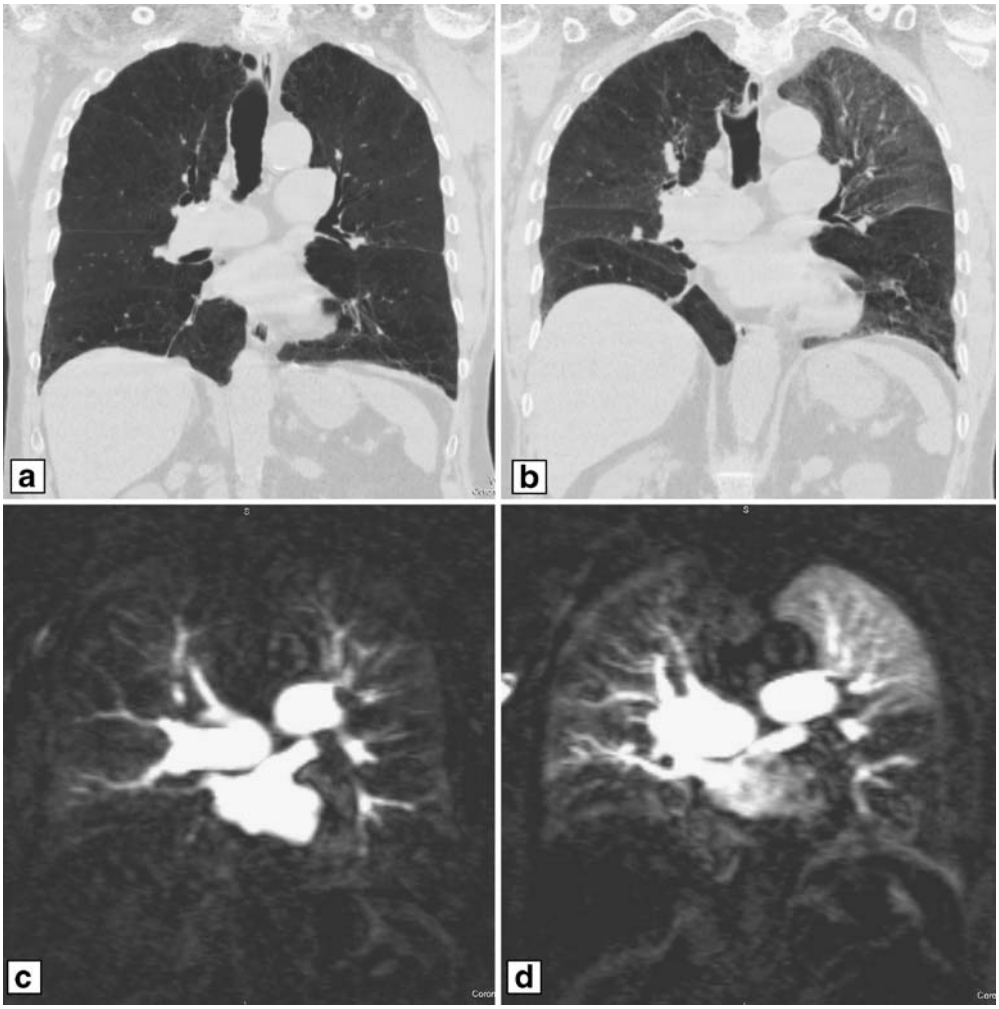

Fig. 7 Coronal CT reformat at maximum inspiration (**a**) and maximum expiration (**b**) presented as 5-mm minimum intensity projection (MinIP): air-trapping in the right and left lower lung, physiological increase in density in the left upper lung in expiration. Corresponding subtracted coronal contrast-enhanced MR perfusion (10-mm MIP): low perfusion at inspiration (**c**) with a distinct increase in particularly in the left upper lung at expiration (**d**)

However, the temporal resolution is less than in MRI and the radiation dose is higher than in non-gated CT scan. No study has reported CT analysis of right ventricular volumes or strain in COPD patients, yet.

MRI

Assessment of right ventricular function using MRI by can be done either by phase contrast flow measurements in the pulmonary trunk or by short axis cine-acquisition of the right ventricle [53]. Thus, early changes of the complex geometry of the right ventricular wall and chamber volume can be accurately measured. In clinically stable, normoxic COPD patients the right ventricular wall mass is significantly higher compared with healthy volunteers, while the ejection fraction was unchanged showing the preserved right ventricular function [53]. The position of the heart is rotated and shifted to a more vertical position in the thoracic cavity due to hyperinflation of the lungs, enlarging the retrosternal space. In COPD patients with hypoxemia, increased right ventricular volumes, decreased right ventricular function, and impaired left ventricular diastolic function were found (Fig. 8) [54].

Ventilation

As sufficient gas exchange depends on matched perfusion and ventilation, assessment of regional ventilation is important for the diagnosis and evaluation of pulmonary emphysema. Traditionally regional lung ventilation is assessed by nuclear medicine examinations. However, these techniques are hampered by low spatial resolution and the necessity of inhalation of a radioactive tracer.

CT

To image ventilation in CT a gaseous contrast agent has to be applied. The most widely used technique is stable, non-radioactive xenon as it provides similar contrast enhance-

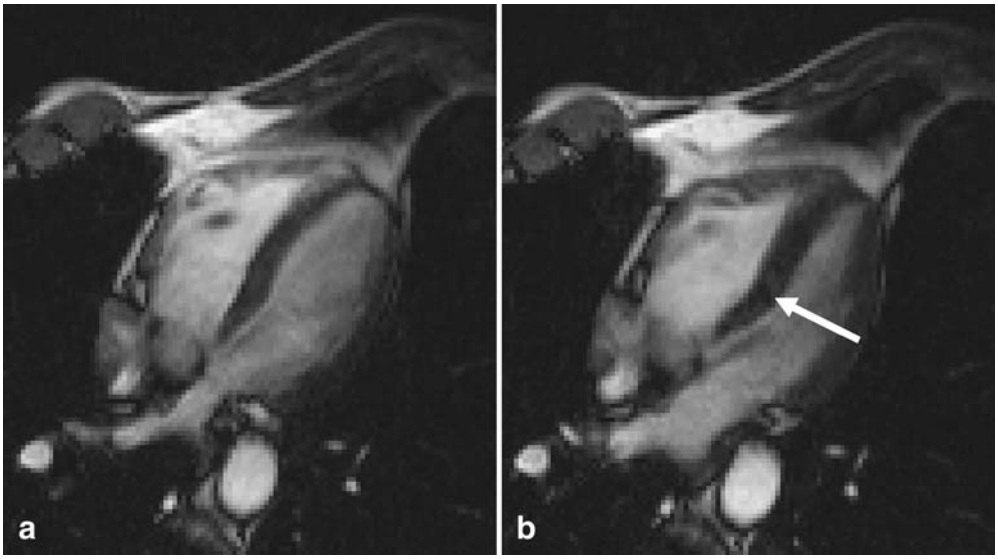

Fig. 8 Four-chamber view in diastole (**a**) and systole (**b**) showing wall thickening of the right myocardium and paradoxic septal movement during systole (*arrow*)

ment as iodine. Regional ventilation is measured from the time course of cine-CT density change during a multibreath wash-in and wash-out of xenon gas. Up to now there are no reports on the clinical use of this technique in COPD patients.

MRI

Visualization of ventilation by MRI is mainly achieved using either oxygen-enhancement or inhalation of hyperpolarized gases.

The technique of oxygen-enhanced MRI has been successfully applied in volunteers. However, only few studies have successfully applied oxygen-enhanced MRI to patients with pulmonary diseases in a clinical setting [55]. It was found that the T1 times of the lung parenchyma are significantly shorter in patients with emphysema [56], leading to a lower signal intensity with heterogeneous distribution compared with volunteers [57].

Ohno et al. [55] found that oxygen-enhanced MR showed that regional changes in ventilation reflected regional lung function. The maximum mean relative enhancement ratio correlated with the diffusion capacity for carbon monoxide (r^2=0.83), while the mean slope of relative enhancement was strongly correlated with the FEV_1 (r^2=0.74) and the maximum mean relative enhancement with the high-resolution CT emphysema score (r^2=0.38) [55]. Oxygen-enhanced MRI requires no special scanner hardware, is easy to use and the costs for oxygen are low. However, the use of high oxygen concentrations (15 l/min) may be risky in patients with severe COPD.

Over the past decade, hyperpolarized noble gas MRI using ^{3}Helium and ^{129}Xenon was developed to improve imaging of pulmonary ventilation. ^{3}Helium has become the most widely used gas for these studies as ^{3}Helium provides higher signal-to-noise ratios than ^{129}Xenon [58]. ^{3}Helium MRI allows for evaluation of static and dynamic gas distribution as well as airspace dimensions (diffusion-weighted imaging). The areas with ventilation defects (due to airway obstruction and emphysema) can not be assessed by dynamic and diffusion-weighted imaging as they rely on the presence of ^{3}Helium. Therefore, they can only provide limited information on the affected lung regions.

Airflow obstruction leads to a reduced level of ^{3}Helium in the distal lung regions, allowing for sensitive detection of ventilation abnormalities (Fig. 9) [59]. In healthy smokers with normal lung function even subtle ventilation defects were visualized, demonstrating the high sensitivity of the technique [60]. Volume of ventilated lung areas on ^{3}He-MRI correlated well with vital capacity (r=0.9) and the amount of non-emphysematous volume on CT (r=0.7) in patients with severe emphysema following single lung transplantation [61]. Quantification of ventilatory impairment can be achieved by automatic segmentation of the lung allowing for precise pre- and post-therapeutic comparison of ventilation [62].

^{3}Helium MRI with high temporal resolution shows the dynamic distribution of ventilation during continuous breathing after inhalation of a single breath of ^{3}Helium gas being capable to demonstrate airflow abnormalities [63, 64]. Homogeneous and fast distribution is regarded as normal, whereas COPD/emphysema patients show irregular and delayed patterns with redistribution and air-trapping [64–66].

The apparent diffusion coefficient (ADC) is a sensitive measure for the airspace size. COPD patients showed increased airspace dimensions compared to non-smokers [67]. ADC images were homogeneous in healthy volunteers, but demonstrated regional variations in emphysema patients. The mean ADCs for emphysema patients

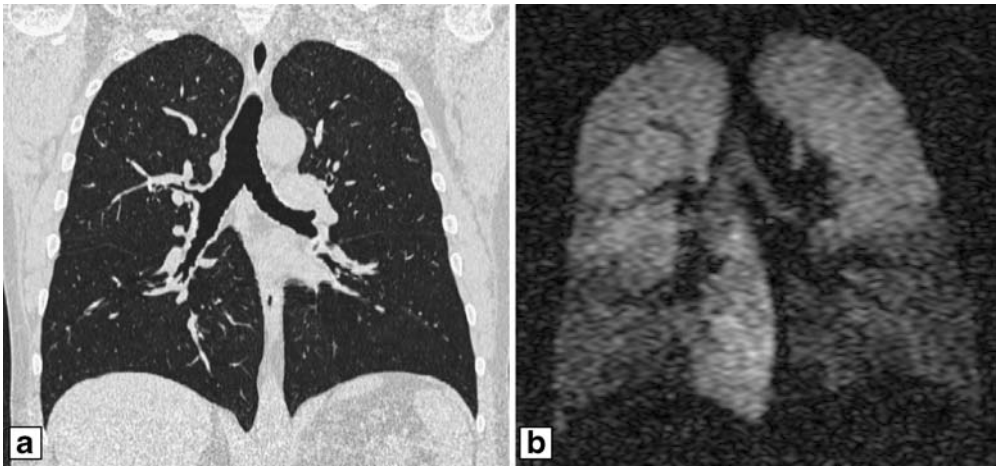

Fig. 9 Coronal CT reformat (**a**) and MR ventilation using hyperpolarized ^{3}Helium gas (**b**). Note only mild emphysema on CT with preserved ventilation in the upper lung but reduced ventilation in left lower and parts of the right lower lung

(0.452 cm^2/cm) were significantly larger ($P<0.002$) than those for volunteers (0.225 cm^2/cm) [68].

Respiratory dynamics

Hyperinflation of the lung severely affects diaphragmatic geometry with subsequent reduction of the mechanical properties, while the effects on the mechanical advantage of the neck and rib cage muscles are less pronounced [69]. The common clinical measurements of COPD do not provide insights into how structural alterations in the lung lead to dysfunction in the breathing mechanics, although treatments such as lung volume reduction surgery (LVRS) are thought to improve lung function by facilitating breathing mechanics and increasing elastic recoil [70]. The complex interaction between chest wall and diaphragmatic motion can be visualized by fluoroscopy. But this technique is limited by the fact being a projection technique.

CT

Cine-CT can be used to assess respiratory dynamics, but generally it is limited to a single table position. New technologies, such as respiratory gated 4D-CT allows for volumetric analysis of motion. As the clinical benefit is unclear, the increased radiation exposure does not seem to be justified for the assessment of COPD.

MRI

Two-dimensional or 3D dynamic MRI is capable to image chest wall and diaphragmatic motion. For data acquisition time resolved techniques with a temporal resolution of 100 ms per frame are used (Figs. 2, 10) [71]. In contrast to normal subjects, patients with emphysema frequently showed reduced, irregular or asynchronous motion of the diaphragm and chest wall, with a significant decrease in the maximum amplitude and the length of apposition of

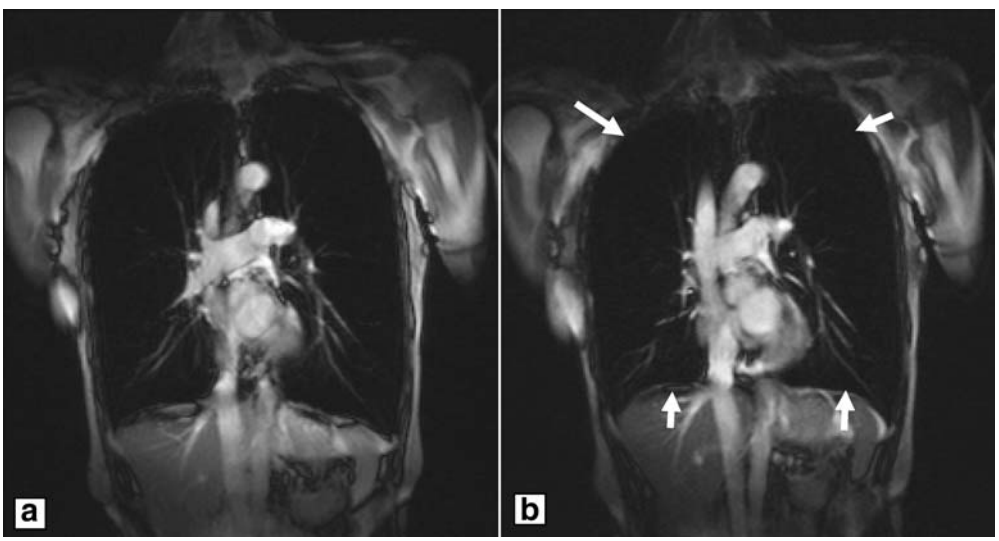

Fig. 10 A 61-year-old female patient suffering from emphysema (FEV_1=0.7l/s, FEV_1 28% predicted). Coronal MR images taken from a dynamic series acquired during forced expiration reflecting maximum inspiration (**a**) and expiration (**b**) show almost complete lack of motion (*arrows*)

the diaphragm [72]. In some patients, the ventral portion of the hemidiaphragm moved downward while the dorsal part moved upward like a seesaw [73]. The paradoxical diaphragmatic motion correlated with hyperinflation, although severe hyperinflation tended to restrict both normal and paradoxical diaphragmatic motion [74]. After lung volume reduction surgery, patients showed improvements in diaphragm and chest wall configuration and mobility [72].

Conclusion

COPD is a heterogeneous disease affecting different regions of the lung with different severity during the course of the disease. The different aspects of COPD need to be assessed by a combination of morphological and functional examinations. Three-dimensional HRCT is the technique of choice for morphological imaging, while MRI allows for comprehensive functional imaging. Inspiratory and expiratory 3D-HRCT with volumetric and texture analysis allows for deeper insights in local hyperinflation and expiratory obstruction. Three-dimensional HRCT is also the "gold standard" for non-invasive quantitative evaluation of airway dimensions. The ability to separate airway predominant from parenchymal predominant pathology in COPD may provide useful information for specific therapies. Recent developments in MRI allow for better visual assessment of the lung morphology. The major advantage of MRI is the assessment of regional lung function including perfusion, respiratory dynamics and ventilation.

References

1. GOLD (2006) Global strategy for the diagnosis, management, and prevention of chronic obstructive pulmonary disease. Executive summery, updated http://www.goldcopd.org
2. Szilasi M, Dolinay T, Nemes Z, Strausz J (2006) Pathology of chronic obstructive pulmonary disease. Pathol Oncol Res 12:52–60
3. Rosenkranz S (2007) Pulmonary hypertension: current diagnosis and treatment. Clin Res Cardiol 96:527–541
4. Ley-Zaporozhan J, Ley S, Kauczor HU (2007) Proton MRI in COPD. Copd 4:55–65
5. Bankier AA, Madani A, Gevenois PA (2002) CT quantification of pulmonary emphysema: assessment of lung structure and function. Crit Rev Comput Tomogr 43:399–417
6. Gevenois PA, De Vuyst P, de Maertelaer V, Zanen J, Jacobovitz D, Cosio MG, Yernault JC (1996) Comparison of computed density and microscopic morphometry in pulmonary emphysema. Am J Respir Crit Care Med 154:187–192
7. Newell JD Jr, Hogg JC, Snider GL (2004) Report of a workshop: quantitative computed tomography scanning in longitudinal studies of emphysema. Eur Respir J 23:769–775
8. Martinez FJ, Foster G, Curtis JL, Criner G, Weinmann G, Fishman A, DeCamp MM, Benditt J, Sciurba F, Make B, Mohsenifar Z, Diaz P, Hoffman E, Wise R (2006) Predictors of mortality in patients with emphysema and severe airflow obstruction. Am J Respir Crit Care Med 173:1326–1334
9. Aziz ZA, Wells AU, Desai SR, Ellis SM, Walker AE, MacDonald S, Hansell DM (2005) Functional impairment in emphysema: contribution of airway abnormalities and distribution of parenchymal disease. AJR Am J Roentgenol 185:1509–1515
10. Nakano Y, Sakai H, Muro S, Hirai T, Oku Y, Nishimura K, Mishima M (1999) Comparison of low attenuation areas on computed tomographic scans between inner and outer segments of the lung in patients with chronic obstructive pulmonary disease: incidence and contribution to lung function. Thorax 54:384–389
11. Bankier AA, De Maertelaer V, Keyzer C, Gevenois PA (1999) Pulmonary emphysema: subjective visual grading versus objective quantification with macroscopic morphometry and thin-section CT densitometry. Radiology 211:851–858
12. Gevenois PA, de Maertelaer V, De Vuyst P, Zanen J, Yernault JC (1995) Comparison of computed density and macroscopic morphometry in pulmonary emphysema. Am J Respir Crit Care Med 152:653–657
13. Baldi S, Miniati M, Bellina CR, Battolla L, Catapano G, Begliomini E, Giustini D, Giuntini C (2001) Relationship between extent of pulmonary emphysema by high-resolution computed tomography and lung elastic recoil in patients with chronic obstructive pulmonary disease. Am J Respir Crit Care Med 164:585–589
14. Stoel BC, Stolk J (2004) Optimization and standardization of lung densitometry in the assessment of pulmonary emphysema. Invest Radiol 39:681–688
15. Madani A, Zanen J, de Maertelaer V, Gevenois PA (2006) Pulmonary emphysema: objective quantification at multi-detector row CT–comparison with macroscopic and microscopic morphometry. Radiology 238:1036–1043
16. Kinsella M, Muller NL, Abboud RT, Morrison NJ, DyBuncio A (1990) Quantitation of emphysema by computed tomography using a "density mask" program and correlation with pulmonary function tests. Chest 97:315–321
17. Arakawa A, Yamashita Y, Nakayama Y, Kadota M, Korogi H, Kawano O, Matsumoto M, Takahashi M (2001) Assessment of lung volumes in pulmonary emphysema using multidetector helical CT: comparison with pulmonary function tests. Comput Med Imaging Graph 25:399–404

18. Zaporozhan J, Ley S, Eberhardt R, Weinheimer O, Iliyushenko S, Herth F, Kauczor HU (2005) Paired inspiratory/expiratory volumetric thin-slice CT scan for emphysema analysis: comparison of different quantitative evaluations and pulmonary function test. Chest 128:3212–3220
19. Boedeker KL, McNitt-Gray MF, Rogers SR, Truong DA, Brown MS, Gjertson DW, Goldin JG (2004) Emphysema: effect of reconstruction algorithm on CT imaging measures. Radiology 232:295–301
20. Ley-Zaporozhan J, Ley S, Weinheimer O, Iliyushenko S, Erdugan S, Eberhardt R, Fuxa A, Mews J, Kauczor HU (2007) Quantitative analysis of emphysema in 3D using MDCT: influence of different reconstruction algorithms. Eur J Radiol DOI 10.1016/j.grad.2007.03.034
21. Madani A, De Maertelaer V, Zanen J, Gevenois PA (2007) Pulmonary emphysema: radiation dose and section thickness at multidetector CT quantification–comparison with macroscopic and microscopic morphometry. Radiology 243:250–257
22. Zaporozhan J, Ley S, Weinheimer O, Eberhardt R, Tsakiris I, Noshi Y, Herth F, Kauczor HU (2006) Multi-detector CT of the chest: influence of dose onto quantitative evaluation of severe emphysema: a simulation study. J Comput Assist Tomogr 30:460–468
23. Mishima M, Hirai T, Itoh H, Nakano Y, Sakai H, Muro S, Nishimura K, Oku Y, Chin K, Ohi M, Nakamura T, Bates JH, Alencar AM, Suki B (1999) Complexity of terminal airspace geometry assessed by lung computed tomography in normal subjects and patients with chronic obstructive pulmonary disease. Proc Natl Acad Sci USA 96:8829–8834
24. Hoffman EA, Simon BA, McLennan G (2006) State of the Art. A structural and functional assessment of the lung via multidetector-row computed tomography: phenotyping chronic obstructive pulmonary disease. Proc Am Thorac Soc 3:519–532
25. Xu Y, Sonka M, McLennan G, Guo J, Hoffman EA (2006) MDCT-based 3-D texture classification of emphysema and early smoking related lung pathologies. IEEE Trans Med Imaging 25:464–475
26. Bankier AA, O'Donnell CR, Mai VM, Storey P, De Maertelaer V, Edelman RR, Chen Q (2004) Impact of lung volume on MR signal intensity changes of the lung parenchyma. J Magn Reson Imaging 20:961–966
27. Hatabu H, Chen Q, Stock KW, Gefter WB, Itoh H (1999) Fast magnetic resonance imaging of the lung. Eur J Radiol 29:114–132
28. Hogg JC, Chu F, Utokaparch S, Woods R, Elliott WM, Buzatu L, Cherniack RM, Rogers RM, Sciurba FC, Coxson HO, Pare PD (2004) The nature of small-airway obstruction in chronic obstructive pulmonary disease. N Engl J Med 350:2645–2653
29. Hogg JC (2006) State of the art. Bronchiolitis in chronic obstructive pulmonary disease. Proc Am Thorac Soc 3:489–493
30. Heussel CP, Ley S, Biedermann A, Rist A, Gast KK, Schreiber WG, Kauczor HU (2004) Respiratory lumenal change of the pharynx and trachea in normal subjects and COPD patients: assessment by cine-MRI. Eur Radiol 14:2188–2197
31. Boiselle PM, Ernst A (2006) Tracheal morphology in patients with tracheomalacia: prevalence of inspiratory lunate and expiratory "frown" shapes. J Thorac Imaging 21:190–196
32. Goldin JG (2002) Quantitative CT of the lung. Radiol Clin North Am 40:145–162
33. Mayer D, Bartz D, Fischer J, Ley S, del Rio A, Thust S, Kauczor HU, Heussel CP (2004) Hybrid segmentation and virtual bronchoscopy based on CT images. Acad Radiol 11:551–565
34. Berger P, Laurent F, Begueret H, Perot V, Rouiller R, Raherison C, Molimard M, Marthan R, Tunon-de-Lara JM (2003) Structure and function of small airways in smokers: relationship between air trapping at CT and airway inflammation. Radiology 228:85–94
35. Hansell DM (2001) Small airways diseases: detection and insights with computed tomography. Eur Respir J 17:1294–1313
36. Park JW, Hong YK, Kim CW, Kim DK, Choe KO, Hong CS (1997) High-resolution computed tomography in patients with bronchial asthma: correlation with clinical features, pulmonary functions and bronchial hyperresponsiveness. J Investig Allergol Clin Immunol 7:186–192
37. Nakano Y, Muller NL, King GG, Niimi A, Kalloger SE, Mishima M, Pare PD (2002) Quantitative assessment of airway remodeling using high-resolution CT. Chest 122:271S–275S
38. Hasegawa M, Nasuhara Y, Onodera Y, Makita H, Nagai K, Fuke S, Ito Y, Betsuyaku T, Nishimura M (2006) Airflow limitation and airway dimensions in chronic obstructive pulmonary disease. Am J Respir Crit Care Med 173:1309–1315
39. Biederer J, Both M, Graessner J, Liess C, Jakob P, Reuter M, Heller M (2003) Lung morphology: fast MR imaging assessment with a volumetric interpolated breath-hold technique: initial experience with patients. Radiology 226:242–249
40. Beckmann N, Cannet C, Zurbruegg S, Rudin M, Tigani B (2004) Proton MRI of lung parenchyma reflects allergen-induced airway remodeling and endotoxin-aroused hyporesponsiveness: a step toward ventilation studies in spontaneously breathing rats. Magn Reson Med 52:258–268
41. Euler US, Liljestrand G (1946) Observation on the pulmonary arterial blood pressuer in the cat. Acta Physiol Scand 12:301–320
42. Cederlund K, Hogberg S, Jorfeldt L, Larsen F, Norman M, Rasmussen E, Tylen U (2003) Lung perfusion scintigraphy prior to lung volume reduction surgery. Acta Radiol 44:246–251
43. Thabut G, Dauriat G, Stern JB, Logeart D, Levy A, Marrash-Chahla R, Mal H (2005) Pulmonary hemodynamics in advanced COPD candidates for lung volume reduction surgery or lung transplantation. Chest 127:1531–1536
44. Sandek K, Bratel T, Lagerstrand L, Rosell H (2002) Relationship between lung function, ventilation-perfusion inequality and extent of emphysema as assessed by high-resolution computed tomography. Respir Med 96:934–943
45. Ley-Zaporozhan J, Ley S, Eberhardt R, Weinheimer O, Fink C, Puderbach M, Eichinger M, Herth F, Kauczor HU (2007) Assessment of the relationship between lung parenchymal destruction and impaired pulmonary perfusion on a lobar level in patients with emphysema. Eur J Radiol 63:76–83
46. Hoffman EA, Chon D (2005) Computed tomography studies of lung ventilation and perfusion. Proc Am Thorac Soc 2:492–498, 506
47. Fink C, Puderbach M, Bock M, Lodemann KP, Zuna I, Schmahl A, Delorme S, Kauczor HU (2004) Regional lung perfusion: assessment with partially parallel three-dimensional MR imaging. Radiology 231:175–184
48. Fink C, Ley S, Kroeker R, Requardt M, Kauczor HU, Bock M (2005) Time-resolved contrast-enhanced three-dimensional magnetic resonance angiography of the chest: combination of parallel imaging with view sharing (TREAT). Invest Radiol 40:40–48

49. Morino S, Toba T, Araki M, Azuma T, Tsutsumi S, Tao H, Nakamura T, Nagayasu T, Tagawa T (2006) Non-invasive assessment of pulmonary emphysema using dynamic contrast-enhanced magnetic resonance imaging. Exp Lung Res 32:55–67
50. Ohno Y, Hatabu H, Murase K, Higashino T, Kawamitsu H, Watanabe H, Takenaka D, Fujii M, Sugimura K (2004) Quantitative assessment of regional pulmonary perfusion in the entire lung using three-dimensional ultrafast dynamic contrast-enhanced magnetic resonance imaging: preliminary experience in 40 subjects. J Magn Reson Imaging 20:353–365
51. Weitzenblum E (1994) The pulmonary circulation and the heart in chronic lung disease. Monaldi Arch Chest Dis 49:231–234
52. Bruzzi JF, Remy-Jardin M, Delhaye D, Teisseire A, Khalil C, Remy J (2006) When, why, and how to examine the heart during thoracic CT: Part 2, clinical applications. AJR Am J Roentgenol 186:333–341
53. Vonk-Noordegraaf A, Marcus JT, Holverda S, Roseboom B, Postmus PE (2005) Early changes of cardiac structure and function in COPD patients with mild hypoxemia. Chest 127:1898–1903
54. Budev MM, Arroliga AC, Wiedemann HP, Matthay RA (2003) Cor pulmonale: an overview. Semin Respir Crit Care Med 24:233–244
55. Ohno Y, Sugimura K, Hatabu H (2003) Clinical oxygen-enhanced magnetic resonance imaging of the lung. Top Magn Reson Imaging 14:237–243
56. Stadler A, Stiebellehner L, Jakob PM, Arnold JF, Bankier AA (2006) [T1 maps and O(2)-enhanced MRT of the diseased lung. Emphysema, fibrosis, mucoviscidosis.]. Radiologe 46:282, 284–9
57. Muller CJ, Schwaiblmair M, Scheidler J, Deimling M, Weber J, Loffler RB, Reiser MF (2002) Pulmonary diffusing capacity: assessment with oxygen-enhanced lung MR imaging preliminary findings. Radiology 222:499–506
58. van Beek EJ, Wild JM, Kauczor HU, Schreiber W, Mugler JP 3rd, de Lange EE (2004) Functional MRI of the lung using hyperpolarized 3-helium gas. J Magn Reson Imaging 20:540–554
59. Kauczor HU, Hofmann D, Kreitner KF, Nilgens H, Surkau R, Heil W, Potthast A, Knopp MV, Otten EW, Thelen M (1996) Normal and abnormal pulmonary ventilation: visualization at hyperpolarized He-3 MR imaging. Radiology 201:564–568
60. Guenther D, Eberle B, Hast J, Lill J, Markstaller K, Puderbach M, Schreiber WG, Hanisch G, Heussel CP, Surkau R, Grossmann T, Weiler N, Thelen M, Kauczor HU (2000) (3)He MRI in healthy volunteers: preliminary correlation with smoking history and lung volumes. NMR Biomed 13:182–189
61. Zaporozhan J, Ley S, Gast KK, Schmiedeskamp J, Biedermann A, Eberle B, Kauczor HU (2004) Functional analysis in single-lung transplant recipients: a comparative study of high-resolution CT, (3)He-MRI, and pulmonary function tests. Chest 125:173–181
62. Ray N, Acton ST, Altes T, de Lange EE, Brookeman JR (2003) Merging parametric active contours within homogeneous image regions for MRI-based lung segmentation. IEEE Trans Med Imaging 22:189–199
63. Salerno M, Altes TA, Brookeman JR, de Lange EE, Mugler JP 3rd (2001) Dynamic spiral MRI of pulmonary gas flow using hyperpolarized (3)He: preliminary studies in healthy and diseased lungs. Magn Reson Med 46:667–677
64. Wild JM, Paley MN, Kasuboski L, Swift A, Fichele S, Woodhouse N, Griffiths PD, van Beek EJ (2003) Dynamic radial projection MRI of inhaled hyperpolarized 3He gas. Magn Reson Med 49:991–997
65. Kauczor HU (2003) Hyperpolarized helium-3 gas magnetic resonance imaging of the lung. Top Magn Reson Imaging 14:223–230
66. Gast KK, Puderbach MU, Rodriguez I, Eberle B, Markstaller K, Knitz F, Schmiedeskamp J, Weiler N, Schreiber WG, Mayer E, Thelen M, Kauczor HU (2003) Distribution of ventilation in lung transplant recipients: evaluation by dynamic 3He-MRI with lung motion correction. Invest Radiol 38:341–348
67. Swift AJ, Wild JM, Fichele S, Woodhouse N, Fleming S, Waterhouse J, Lawson RA, Paley MN, Van Beek EJ (2005) Emphysematous changes and normal variation in smokers and COPD patients using diffusion 3He MRI. Eur J Radiol 54:352–358
68. Salerno M, de Lange EE, Altes TA, Truwit JD, Brookeman JR, Mugler JP 3rd (2002) Emphysema: hyperpolarized helium 3 diffusion MR imaging of the lungs compared with spirometric indexes–initial experience. Radiology 222:252–260
69. Decramer M (1997) Hyperinflation and respiratory muscle interaction. Eur Respir J 10:934–941
70. Henderson AC, Ingenito EP, Salcedo ES, Moy ML, Reilly JJ, Lutchen KR (2007) Dynamic lung mechanics in late-stage emphysema before and after lung volume reduction surgery. Respir Physiol Neurobiol 155:234–242
71. Plathow C, Klopp M, Fink C, Sandner A, Hof H, Puderbach M, Herth F, Schmahl A, Kauczor HU (2005) Quantitative analysis of lung and tumour mobility: comparison of two time-resolved MRI sequences. Br J Radiol 78:836–840
72. Suga K, Tsukuda T, Awaya H, Takano K, Koike S, Matsunaga N, Sugi K, Esato K (1999) Impaired respiratory mechanics in pulmonary emphysema: evaluation with dynamic breathing MRI. J Magn Reson Imaging 10:510–520
73. Iwasawa T, Yoshiike Y, Saito K, Kagei S, Gotoh T, Matsubara S (2000) Paradoxical motion of the hemidiaphragm in patients with emphysema. J Thorac Imaging 15:191–195
74. Iwasawa T, Kagei S, Gotoh T, Yoshiike Y, Matsushita K, Kurihara H, Saito K, Matsubara S (2002) Magnetic resonance analysis of abnormal diaphragmatic motion in patients with emphysema. Eur Respir J 19:225–231